Studies on an Argon Laser-Induced Photopolymerization Employing Both Mono- and Bischromophoric Hemicyanine Dye—Borate Complex as a Photoinitiator. Part III

Beata Jędrzejewska, Sławomir Urbański*

Faculty of Chemical Technology and Engineering, University of Technology and Life Sciences, Seminaryjna 3, 85-326 Bydgoszcz, Poland

Received 13 July 2009; accepted 1 March 2010
DOI 10.1002/app.32348
Published online 3 June 2010 in Wiley InterScience (www.interscience.wiley.com).

ABSTRACT: Two series of homodimeric hemicyanine dyes based on 4-(*p*-*N*,*N*-dialkylaminostyryl)pyridinium and 4-(*p*-*N*,*N*-dialkylaminostyryl)quinolinium residues have been evaluated as novel photoinitiators for radical polymerization induced with an argon ion laser visible emission. In the tested photoredox pairs, hemicyanine dye cation acts as an electron acceptor and it is coupled with *n*-butyltriphenyl borate anion being an electron donor. The photochemistry of the series of bichromophoric stilbazolium borates, 1,3-, 1,5-, and 1,10-bis-[4-(*p*-*N*,*N*-dialkylaminostyryl)pyridinyl]alkane di-*n*-butyltriphenylborates and 1,3-, 1,5-, and 1,10-bis-[4-(*p*-*N*,*N*-dialkylaminostyryl) quinolinyl]alkane di-*n*-butyltriphenylborates, was compared with the photochemistry of the structurally related, monochromophoric styrylpyridinium and the styrylquinolinium borates. The experimental results indicated that the rate of photopolymerization depends on ΔG_{el} of the electron transfer between borate anion and hemicyanine cation. The relationship between the rate of polymerization and the free energy of activation shows the dependence predicted by the classical theory of the electron transfer. © 2010 Wiley Periodicals, Inc. J Appl Polym Sci 118: 1395–1405, 2010

Key words: dyes; initiators; radical polymerization; differential scanning calorimetry (photo-DSC)

INTRODUCTION

Photopolymerization science and technology have assumed an increasing relevance in many applications. This technology is based on the use of photoinitiator systems suited to absorbing photons to produce primary radical species, which are able to initiate polymerization.[1–5] Photoinitiated radical polymerization may be initiated by both cleavage (Type I) and bimolecular type of initiators (Type II, electron transfer and H-abstraction reactions).[1] Type I photoinitiators undergo a cleavage process to form two radical species. Type II photoinitiators are based on a bimolecular reaction with either electron or hydrogen donors to produce initiating radicals. Typical Type II photoinitiators are benzophenone and its derivatives, thioxanthones, benzil, quionones, and organic dyes, while alcohols, ethers, amines and thiols are used as the hydrogen donors[6–8] and borate anions or a wide group of carboxylic acids are applied as the electron donors.[9–11]

Interesting examples are borate salt initiators. They work by inter- or intramolecular photoinduced electron transfer (PET).[12–17] In case of the cyanine borate the polymerization is initiated by an alkyl radical formed as a result of the PET from borate anion to the excited state of cyanine dye, followed by a rapid cleavage of the alkyl boron bond of the boranyl radical (Fig. 1).

Application of cyanine dye borate salts as photoinitiating systems gives an opportunity to change the usefulness of irradiation region of these photoinitiators by changing the structure of the cyanine dye. The modification of the dye structure by shortening or extending a polymethine chain, by introduction different substituents in heterocyclic moiety or in the "meso" position of polymethine chain leads to the changes in absorption spectra and in the efficiency of the radical polymerization of vinyl monomers.[14] From our earlier studies, it is known that the modification of the hemicyanine dye structure by introduction of the second, not conjugated with the dye molecule, quaternary nitrogen significantly enhances the efficiency of the photoinitiation.[15–17]

In this study, photophysical characteristics of the photoinitiating systems consisting of different bichromophoric hemicyanine dyes (the light absorbers) coupled with butyltriphenylborate anions (coinitiators) were determined. The dyes under the study

Correspondence to: B. Jędrzejewska (beata@utp.edu.pl).
*Master degree student.
Contract grant sponsor: State Committee for Scientific Research (KBN); contract grant number: N N204 054135.

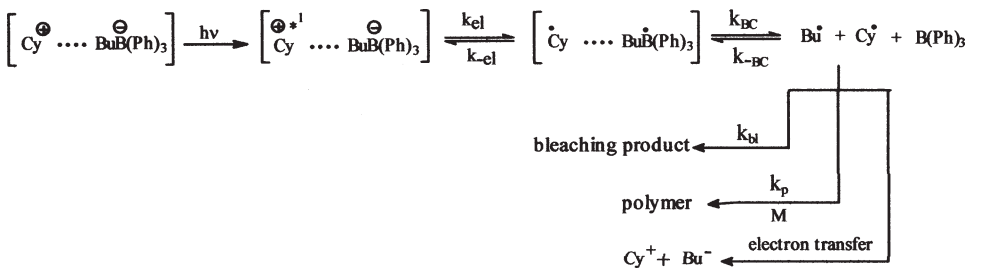

Figure 1 The processes that may occur during the free-radical photoinduced polymerization with the use of cyanine borate initiator; k_{BC} denotes the rate of carbon-boron bond cleavage, k_{-BC} describes the reverse step, and k_{bl} is the rate constant of free radical crosscoupling step yielding bleached dye.

were used in the radical polymerization of multifunctional monomer and the results obtained were compared with the photopolymerization results of the monochromophoric hemicyanine dyes.

EXPERIMENTAL

Materials

Monomer, 2-ethyl-2-(hydroxymethyl)-1,3-propanediol triacrylate (TMPTA), 1-methyl-2-pyrrolidinone (MP), and the spectroscopic grade solvents for spectral measurements were purchased from Aldrich Chemical Co. and were used without further purification. Dye photoinitiators were synthesized in our laboratory according to procedures described in the literature.[18–20]

The molecular structure and the denotations of the dyes under the study are given in Chart 1.

Spectral measurements

The absorption spectra were recorded with a Shimadzu UV–Vis Multispec-1501 spectrophotometer and fluorescence spectra were obtained with a Hitachi F-4500 spectrofluorimeter. The fluorescence measurements were performed at an ambient temperature.

Electrochemical measurements

The reduction potentials of the dyes (P1-P8 and D1-D8) and the oxidation potential of tetramethylammonium *n*-butyltriphenylborate (TB2) were measured by cyclic voltammetry using an Electroanalytical Cypress System Model CS-1090. A platinum 1-mm disk electrode was used as the working electrode, a Pt wire constituted the counter electrode, and Ag-AgCl electrode served as a reference electrode. The supporting electrolyte was 0.1*M* tetra-*n*-butylammonium perchlorate in a dry acetonitrile.

Polymerization measurements

The kinetics of the radical polymerization was studied using a polymerization solution composed of 1 mL of 1-methyl-2-pyrrolidinone (MP) and 9 mL of 2-ethyl-2-(hydroxymethyl)-1,3-propanediol triacrylate (TMPTA). The mono- and dicationic hemicyanine borates concentration was 5×10^{-4} *M* for series P and 1×10^{-3} *M* for series D, respectively (calculated for one (single) absorbing chromophore). As a reference sample a polymerizing mixture containing hemicyanine iodide (a dye without an electron donor) was used instead of the hemicyanine borate salt (photoinitiator). The measurements were carried out at an ambient temperature and the polymerizing mixture was not deaerated before curing.

The kinetics of radical polymerization was measured according to the measurements of the rate of the heat evolution during polymerization in a thin film cured sample (0.035 ± 0.002 g; 1-mm thick layer). The measurements were performed by measuring photopolymerization exotherms using photo-DSC apparatus constructed on the basis of a TA Instruments DSC 2010 differential scanning calorimeter. Irradiation of the polymerization mixture was carried out using the emission (line at 514 nm) of an argon ion laser Model Melles Griot 43 series with intensity of the light equal of 100 mW/cm^2. The light intensity was measured by a Coherent Model Fieldmaster power meter. An average value of the rate of polymerization was established based on measurements performed at least three times.

The rate of polymerization (R_p) was calculated using the formula (1) where dH/dt is maximal heat flow during reaction and $\Delta H_p^{\text{theor}}$ is the theoretical enthalpy for complete conversion of acrylates' double bonds. $\Delta H_p^{\text{theor}}$ for acrylic double bond equals 78.2 kJ/mol.[21]

$$R_p = \left(\frac{dH}{dt}\right)\frac{1}{\Delta H_p^{\text{theor}}} \quad (1)$$

RESULTS AND DISCUSSION

Spectroscopic and electrochemical properties

For the analysis of the properties of the novel photoinitiating photoredox pairs the combinations of *n*-

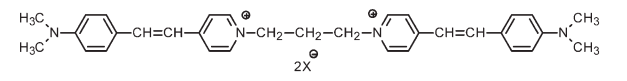

X: I – P1; n-$C_4H_9B(C_6H_5)_3$ – P1B2

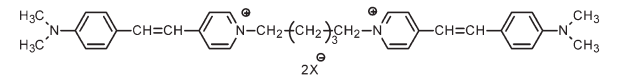

X: I – P2; n-$C_4H_9B(C_6H_5)_3$ – P2B2

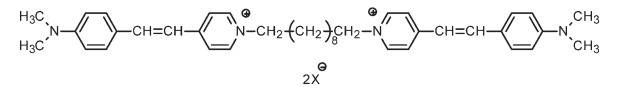

X: I – P3; n-$C_4H_9B(C_6H_5)_3$ – P3B2

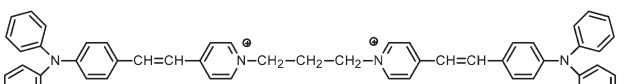

X: I – P4; n-$C_4H_9B(C_6H_5)_3$ – P4B2

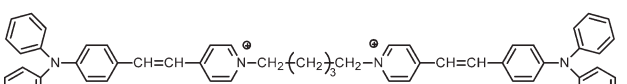

X: I – P5; n-$C_4H_9B(C_6H_5)_3$ – P5B2

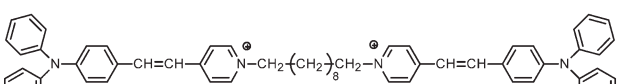

X: I – P6; n-$C_4H_9B(C_6H_5)_3$ – P6B2

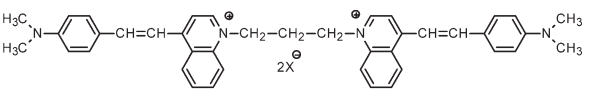

X: I – D1; n-$C_4H_9B(C_6H_5)_3$ – D1B2

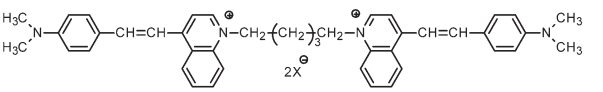

X: I – D2; n-$C_4H_9B(C_6H_5)_3$ – D2B2

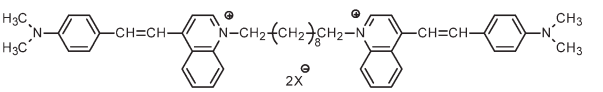

X: I – D3; n-$C_4H_9B(C_6H_5)_3$ – D3B2

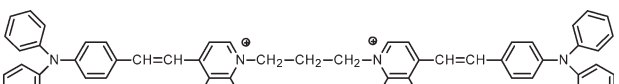

X: I – D4; n-$C_4H_9B(C_6H_5)_3$ – D4B2

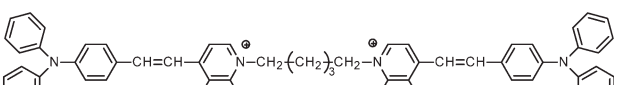

X: I – D5; n-$C_4H_9B(C_6H_5)_3$ – D5B2

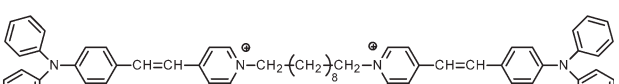

X: I – D6; n-$C_4H_9B(C_6H_5)_3$ – D6B2

Monocationic hemicyanine dyes used for comparison:

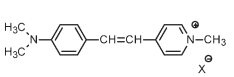

X: I – P7; n-$C_4H_9B(C_6H_5)_3$ – P7B2

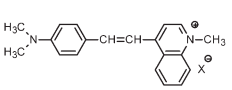

X: I – D7; n-$C_4H_9B(C_6H_5)_3$ – D7B2

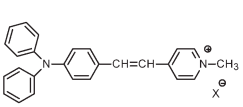

X: I – P8; n-$C_4H_9B(C_6H_5)_3$ – P8B2

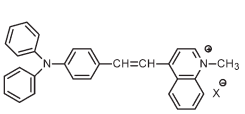

X: I – D8; n-$C_4H_9B(C_6H_5)_3$ – D8B2

Chart 1 (A) Dicationic hemicyanine salts tested as photoinitiators for free-radical polymerization of vinyl monomers. (B) Monocationic hemicyanine dyes used for comparison.

butyltriphenylborate anion (**B2**) and dicationic hemicyanine dyes were used. The structures of all of them are shown in Chart 1.

Bichromophoric hemicyanine dyes under the study are the series of initiators with symmetric molecular structure of a type D-π-A-S-A-π-D, where D and A are an electron donor and an electron acceptor, respectively, and S denotes spacer—alkyl group. The dyes display several specific properties that are similar to the properties of the other styryl dyes reported in the literature.[22–25] They have a common structural feature, namely, possess an electron donor and electron acceptor moiety located on the opposite sides of a styryl double bond. Two positive charges in one hemicyanine dye molecule differentiate the dyes under the study from those commonly recognized as hemicyanine dyes.

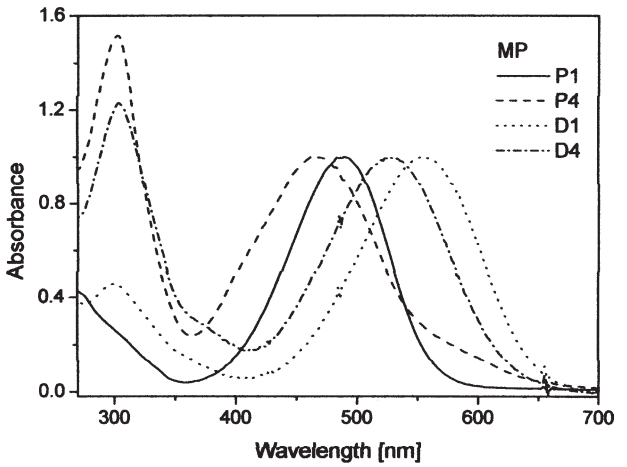

Figure 2 Normalized electronic absorption spectra of selected dyes in MP at 293 K.

Figures 2 and 3 show the illustrative electronic absorption and the fluorescence emission spectra recorded for selected hemicyanine dye in different solvents.

Table I collects the values of the absorption and fluorescence maxima positions and Stokes shifts for all tested dyes in different solvents. For comparison, the data for monocationic hemicyanine dye is presented as well.

The UV–Vis spectroscopic measurements of the tested dimers (Fig. 2) show broad absorption bands in the range of 460–560 nm corresponding to the $S_0 \rightarrow$ CT transition attributed to an intramolecular charge transfer (ICT) involving the electron lone pair of the amino nitrogen and the cationic pyridinium (or quinolinium) nitrogen moiety.[20] The shortest wavelength bands are attributed to the $\pi \rightarrow \pi^*$ transitions. The molar absorption coefficients of the CT bands oscillate between 9400 and 75,000 M^{-1} cm^{-1} for series D and between 15,000 and 100,000 M^{-1} cm^{-1} for series P, respectively. The molar absorption coefficients of shortest wavelength bands range from 12,000 to 67,000 M^{-1} cm^{-1} for series D and from 20,000 and 48,000 M^{-1} cm^{-1} for series P, respectively.[20] Generally, the molar absorption coefficient of the tested dicationic dyes is about twice as high as measured for their monomeric equivalents.[20]

From Table I, it can be also seen that the maximum of the fluorescence spectra for all chromophores are also solvent dependent.

It is also observed (Table I), that the precursor dye, e.g. monocationic dye (**P7**) (1-methyl-4-(4-N,N-dimethylaminostyryl)pyridinium iodide) shows in MP the absorption band with the maximum located at 475 nm, while its dicationic equivalents show the absorption bands with the maxima shifted to the red of about 8–10 nm. The mechanism causing the red shift observed for the dicationic dyes in comparison with its monomeric equivalent is not clear. It may be speculated that the pyridinium (or quinolinium) cation, being in proximity to light absorbing chromophore, causes a substantial increase of the Onsager's cavity radius that affects the solvatochromic behavior of the dyes.[20]

The absorption and emission spectra of tested dyes are visibly affected by the nature of organic solvent. In general, there is a weak blue shift observed in absorption maxima of dyes tested with increasing of a solvent polarity (Table I). The compounds under the study are ionic dyes, which exhibit a dipolar character in the ground state. The solvent molecules are oriented in such a way as required by the dipolar character of the host molecule. During the transition, which occurs within a very small time interval, only the electrons have a time to change position. The excited molecules, in which the electric dipole has been weakened and has been reoriented, are now within a solvent cage that is no longer adopted to the electronic requirements of the excited molecule, since the solvent cage is suitable for the electronic distribution in the ground state molecule. Thus, a polar solvent creates a stabilizing solvent cage around these ionic dyes in the ground state, but a destabilizing solvent cage for the excited state. The transition energy rises with increasing solvent polarity. An increase in the solvent polarity results in a hypsochromic shift of the charge transfer band, i.e., to the shorter wavelengths.

The absorption and the emission spectra of the tested dyes are sensitive to the solvent that is attributed to the difference in the dipole moment in the ground and excited states. The spectra show considerable spectral shifts in the applied organic solvents. The difference in energy between the absorbed and emitted radiation is known as the Stokes shift.[26] The Stokes shift ($\nu_{ab}-\nu_{fl}$), is one of the quantitative

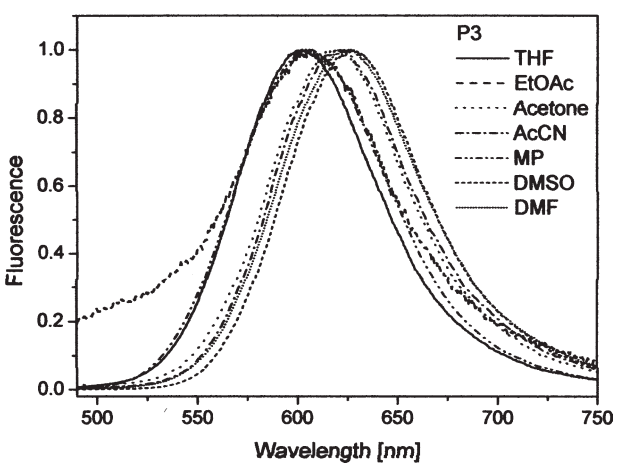

Figure 3 Normalized fluorescence spectra of P3 recorded in solvents of different polarity at 293 K (λ_{ex} = 480 nm).

TABLE I
Steady State Spectroscopic Properties of the Homodicationic Hemicyanine Dyes Under the Study

Dye	Solvent	λ^{ab}_{max} (nm)		λ^{fl}_{max} (nm)	$\Delta\nu$ (cm^{-1})	Dye	λ^{ab}_{max} (nm)		λ^{fl}_{max} (nm)	$\Delta\nu$ (cm^{-1})
P1	MP	–	486	623	4525	D1	301	555	690	3525
	DMSO	275	490	631	4560		307	555	706	3854
	DMF	–	490	632	4585		305	551	699	3843
	Acetone	–	488	625	4492		–	549	698	3888
	Acetonitrile	–	489	629.6	4567		307	556	705	3801
	Chloroform						308	566	652	2330
	EtOAc	299	476	597	4258		295	361 556	668	3016
	THF	299	360 478	601	4282		300	559	685	3291
P2	MP	–	483	620	4575	D2	301	557	695	3565
	DMSO	272	478	624.6	4910		307	554	707.2	3910
	DMF	–	478	625	4921		306	552	700	3830
	Acetone	–	481.5	619	4613		–	547.5	693.2	3839
	Acetonitrile	–	478	622	4843		306	545	705	4164
	Chloroform						306	559	648	2457
	EtOAc	295	369 478	595	4114		–	332 543	674	3579
	THF	299	480	603	4250		301	555	681	3334
P3	MP	–	482	619	4592	D3	304	553	694	3674
	DMSO	273	479	626	4825		305	551	704	3944
	DMF	–	477	624	4939			547	699	3975
	Acetone	–	480	620	4704		–	550	697	3835
	Acetonitrile	–	477	623	4913		305	546	698	3988
	Chloroform						307	565	659	2525
	EtOAc	294	368 478	591	4000		–	330 554	689	3537
	THF	299	366 484	605	4132		300	557	686	3376
P4	MP	303	465	663	6422	D4	304	528	745	5517
	DMSO	303	470	677	6506		306	524	768	6063
	DMF	302	472	694	6777		303	522	774	6237
	Acetone	–	478	705	6736		–	524.5	770	6079
	Acetonitrile	300	478	715	6934		305	529	784	6148
	Chloroform						307	560	710	3773
	EtOAc	295	358 468	653	6054		295	358 528	713	4914
	THF	298	366 470	657	6056		301	539	752	5255
P5	MP	302	465	678	6756	D5	304	528	728	5203
	DMSO	302	465	693	7075		308	524	758	5891
	DMF	302	467	691	6941		306	521	764	5789
	Acetone	–	466	697	7112		–	521	748	5825
	Acetonitrile	301	467	712	7368		302	530	781	6064
	Chloroform						307	555	705	3834
	EtOAc	295	355 471	647	5775		296	348 544	729	4665
	THF	299	366 472	666	6171		301	543	749	5065
P6	MP	302	464	673	6693	D6	302	523	731	5441
	DMSO	303	465	695	7117		305	526	740	5498
	DMF	304	462	691	7173		306	522	716	5191
	Acetone	–	465	697	7112		–	524	712	5039
	Acetonitrile	301	467	712	7368		301	523	771	6150
	Chloroform						306	555	701	3753
	EtOAc	295	357 467	651	6052		295	359 527	703	4751
	THF	299	365 471	658	6034		–	536	731	4977
P7	MP	–	474	621	4994	D7	303	547	690	3789
	DMSO	272	472	625	5186		305	544	706.2	4222
	DMF	–	472	624	5161		304	540	697	4171
	Acetone	–	474	621	4994		–	540	694	4109
	Acetonitrile	301	472	622.2	5114		306	542	697	4103
	Chloroform						306	563	654	2471
	EtOAc	293	365 470	600	4610		297	550	684	3562
	THF	295	367 471	606	4730		301	555	690	3525
P8	MP	303	462	679	6917	D8	304	519	766	6213
	DMSO	302	455	692	7527		306	513	770	6506
	DMF	303	457	693	7452		305	517	776	6456
	Acetone	–	463	698	7272		–	518	775	6402
	Acetonitrile	300	461	714	7686		302	514	795	6877
	Chloroform						308	558	718	3994
	EtOAc	295	364 458	637	6135		297	348 512	712	5486
	THF	298	367 462	655	6378		–	540	756	5291

parameter which is useful to understand the origin of the variation of the spectral shift in organic solvents.

The Lippert equation is a simple and the most widely used expression to explain the general solvent effects (due to the dielectric constant (ε) and the refractive index (n) of the solvent). The Stokes shift is dependent on the orientational polarizability of a solvent (Δf), which is linearly related to this. The Stokes shift values obtained for the homodicationic hemicyanine dyes tested are also given in Table I. The highest values of Stokes shift are observed in polar solvents, and the lowest in chloroforme. The value of Stokes shift depends on the dye structure as well.

The application of the Lippert and Mataga theory allows to understand better the observed properties.[26–29] According to this theory, the specific solvent effects can be expressed by two equations. The first eq. (2) describes the behavior of the absorption band by the following expression:

$$hc\overline{\nu}_{ab}^{CT} \cong hc\overline{\nu}_{ab}^{vac} = \frac{2\vec{\mu}_g(\vec{\mu}_e - \vec{\mu}_g)}{a_0^3} \cdot \left[\frac{\varepsilon - 1}{2\varepsilon + 1} - \frac{1}{2} \cdot \frac{n^2 - 1}{2n^2 + 1}\right] \quad (2)$$

where $hc\overline{\nu}_{ab}^{CT}$ and $hc\overline{\nu}_{ab}^{vac}$ are the energies related to the spectral position of the CT absorption maxima in solution and to the value extrapolated to the gas-phase, respectively; $\vec{\mu}_g$ and $\vec{\mu}_e$ are the dipole moments of the solute in the ground and the excited state; a_0 is the effective radius of the Onsager's cavity, ε is the static dielectric constant, and n is the refractive index of the solvent.

The second eq. (3) describing the solvatochromic effect on the spectral position of the CT fluorescence spectra is given by:

$$hc\overline{\nu}_{fl}^{CT} \cong hc\overline{\nu}_{fl}^{vac} = \frac{2\vec{\mu}_e(\vec{\mu}_e - \vec{\mu}_g)}{a_0^3} \cdot \left[\frac{\varepsilon - 1}{2\varepsilon + 1} - \frac{1}{2} \cdot \frac{n^2 - 1}{2n^2 + 1}\right] \quad (3)$$

where $hc\overline{\nu}_{fl}^{CT}$ and $hc\overline{\nu}_{fl}^{vac}$ are the spectral positions of the solvent equilibrated CT fluorescence bands maxima and the value extrapolated to the gas-phase correspondingly.

The analysis of the trends presented for all dyes allows to conclude that: (i) the negative value of $2\vec{\mu}_g(\vec{\mu}_e - \vec{\mu}_g)$ term suggests that for the Franck–Condon transition $\vec{\mu}_e < \vec{\mu}_g$; (ii) the positive value of $2\vec{\mu}_e(\vec{\mu}_e - \vec{\mu}_g)$ term allows to conclude that for relaxing molecules $\vec{\mu}_e > \vec{\mu}_g$.

Combination of the relationships mentioned above indicates the following possibilities:

(a) The dipole moment of the ground state, from which the molecule is excited, is different from that from which the excited molecule relaxes;
(b) The emission occurs from the molecule with dipole moment different from that obtained after the Franck–Condon excitation; and
(c) The emission occurs from the molecule characterized by the dipole moment different from that from which is excited.

The analysis of the possible spherical conformers of the dyes under the study cannot exclude any of the mentioned above possibilities.

Figure 4 shows the plots of ($\nu_{ab} - \nu_{fl}$) versus the solvent polarity parameter[26] for selected dyes. The plots show linear correlation that is in good agreement with the Lippert–Mataga equation:[26–28]

$$(\nu_{ab} - \nu_{fl}) = \frac{2(\mu_e - \mu_g)^2}{hca^3}\left(\frac{\varepsilon - 1}{2\varepsilon + 1} - \frac{n^2 - 1}{2n^2 + 1}\right) + K \quad (4)$$

where K is a constant.

A linear dependence of the Stokes shift as a function of Δf for all solvents (as shown in Fig. 4) validates the Lippert–Mataga equation and confirms that the dye has a single structure in the ground and the excited states. The slope of the linear relationship depends on the change in the dipole moment caused by the excitation. This correlation predicts also that the Stokes shift should linearly increase with the orientational polarizability.[29] In all tested dyes a linear correlation, with satisfactory coefficient fit ($R^2 \approx$ 0.90–0.97), between Stokes shift and Δf was observed for all solvents used. The results obtained indicate that the excited state dipole moments of hemicyanine dyes under the study should have higher values than those calculated for the ground state (positive slopes of ($\nu_{ab} - \nu_{fl}$) versus the solvent polarity parameter).

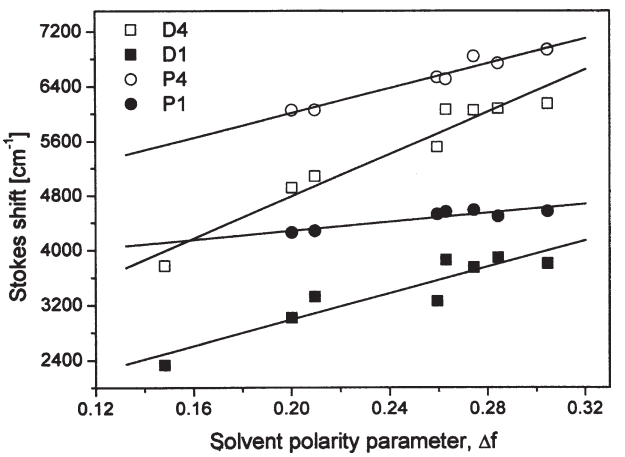

Figure 4 The relationship between the Stokes shift and the solvent polarity parameter, Δf for selected dyes (marked in the figure).

TABLE II
Reduction and Oxidation Potential Data, Energy of the Excited State Involved in Electron Transfer Reaction, Calculated Free Energies (ΔG_{el}) of the Electron Transfer Reaction Between the Singlet Excited State of the Dyes and Electron Donor Tested and the Rate of Photoinitiated Polymerization

Dye	E_{00}[a] (eV)	E_{00}[b] (eV)	E_{00}[c] (eV)	E_{red} (V)	ΔG_{el}[a] (eV)	ΔG_{el}[b] (eV)	ΔG_{el}[c] (eV)	R_p (μmol/s)	σ[d]	$1 + \ln R_p$[e] (au)
P1	2.30	2.22	2.22	−0.766	−0.392	−0.310	−0.316	0.812	0.032	3.015
P2	2.31	2.24	2.24	−0.758	−0.409	−0.338	−0.341	0.939	0.029	3.159
P3	2.28	2.24	2.25	−0.762	−0.376	−0.342	−0.353	0.586	0.006	2.688
P4	2.27	2.20	2.26	−0.714	−0.421	−0.342	−0.408	1.697	0.030	3.751
P5	2.31	2.24	2.23	−0.7	−0.474	−0.396	−0.395	0.648	0.016	2.789
P6	2.25	2.24	2.26	−0.698	−0.411	−0.398	−0.424	0.383	0.036	2.263
P7	2.29	2.29	2.26	−0.79	−0.364	−0.355	−0.328	0.225	0.033	1.733
P8	2.31	2.25	2.27	−0.798	−0.368	−0.310	−0.335	0.108	0.054	1.000
D1	1.99	1.95	1.96	−0.664	−0.392	−0.150	−0.153	0.511	0.062	2.989
D2	2.00	1.95	1.96	−0.636	−0.187	−0.177	−0.184	0.685	0.080	3.281
D3	1.96	1.97	1.99	−0.638	−0.221	−0.189	−0.207	0.461	0.009	2.886
D4	2.05	2.15	2.03	−0.632	−0.180	−0.380	−0.259	0.936	0.041	3.594
D5	1.99	1.98	1.97	−0.644	−0.278	−0.198	−0.191	1.149	0.168	3.799
D6	2.01	2.01	2.05	−0.738	−0.128	−0.134	−0.168	0.946	0.064	3.605
D7	1.98	1.99	1.99	−0.712	−0.224	−0.133	−0.141	0.070	0.000	1.000
D8	2.03	2.12	2.06	−0.788	−0.127	−0.192	−0.133	0.497	0.093	2.962

The oxidation potential of tetramethylammonium *n*-butyltriphenylborate is equal to 1.14 V.
[a] Measured in EtOAc as a solvent.
[b] Measured in DMF as a solvent.
[c] Measured in AcCN as a solvent.
[d] Standard deviation for the polymerization data.
[e] Calculated as a natural logarithm from the quotient of the rate of polymerization for given initiator to the lowest rate of polymerization for the given series enlarged about one.

Generally, we observe a weak negative solvatochromism in the absorption (blue-shift in absorption with increasing polarity of the solvent), a positive solvatochromism in the emission (red-shift in the emission with increasing polarity of solvents).

Discussion on the solvent-dependent spectroscopic properties of the tested dyes presented above suggests that the energy of singlet state on which the electron transfer from an electron donor occurs may be strongly affected by the polarity of a solvent. This, in turn, may have an effect on the value of free energy change for electron transfer process predicted by Rehm–Weller equation.[30]

It is well known that the main prerequisite for the electron transfer (PET) reaction, vital for free radicals formation, states that the thermodynamic driving force of the electron transfer reaction between the excited state of the dye and electron donor should have negative value. The free energy of activation for the PET (ΔG_{el}) process can be easily estimated on the basis of the Rehm–Weller[27] eq. (5):

$$\Delta G_{el} = E_{ox}(D/D^{\cdot+}) - E_{red}(A^{\cdot-}/A) - E_{00} - Ze^2/\varepsilon a \quad (5)$$

where E_{ox} $(D/D^{\cdot+})$ is the oxidation potential of the electron donor, E_{red} $(A^{\cdot-}/A)$ is the reduction potential of the electron acceptor, E_{00} is the energy of the excited state involved in electron transfer reaction (calculated from the intersection of the normalized absorption and the fluorescence spectra recorded in the same solvent), and $Ze^2/\varepsilon a$ is the Coulombic energy associated with the process. Since the last term is relatively small in polar or medium polarity media, it can be neglected in the estimation of ΔG_{el}. The E_{ox} and E_{red} of both photoredox pair components were determined from the cyclovoltametric measurements (Table II). The electrochemical reduction of the dyes is, as it is shown in Figure 5, reversible. However, the oxidation of the tetramethylammonium *n*-butyltriphenylborate is irreversible because of a very short lifetime of alkyltriphenylboranyl

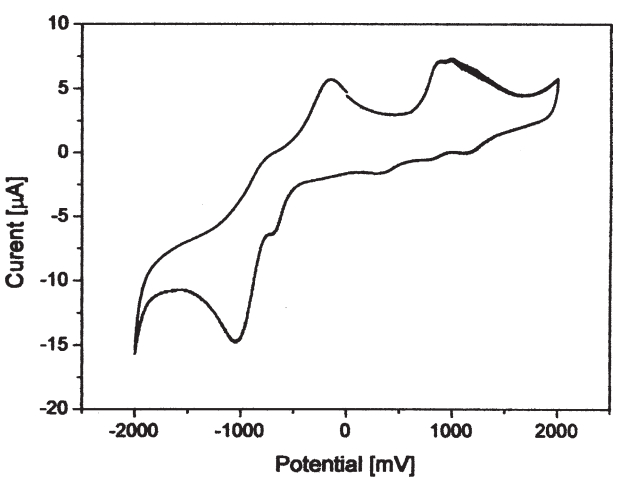

Figure 5 Cyclic voltammogram of D1 in 0.1*M* tetrabutylammonium perchlorate solution in dry acetonitrile as the supporting electrolyte.

radical. Therefore, the obtained electrochemical values for both components of photoredox pairs may have only approximate thermodynamic meaning yet, allow roughly estimate the free energy of activation (ΔG_{el}) for the PET process.

The measured values of the dyes reduction potentials, the electron donor (tetramethylammonium *n*-butyltriphenylborate) oxidation potential ($E_{ox} = 1.14$ V) and the singlet state energy of the dyes, allow one to calculate (using the Rehm–Weller equation[30]) the free energy change for the photoinduced intermolecular electron transfer process. The estimated data are summarized in Table II.

The values of ΔG_{el} of tested photoinitiating systems oscillate in the range from -0.127 to -0.474 eV. The calculations clearly show that for the tested photoredox pairs the electron transfer process is thermodynamically allowed. This, in turn, allows to predict that the tested dyes in combination with borate anion should effectively generate free radical that can start the polymerization of the acrylic monomers.

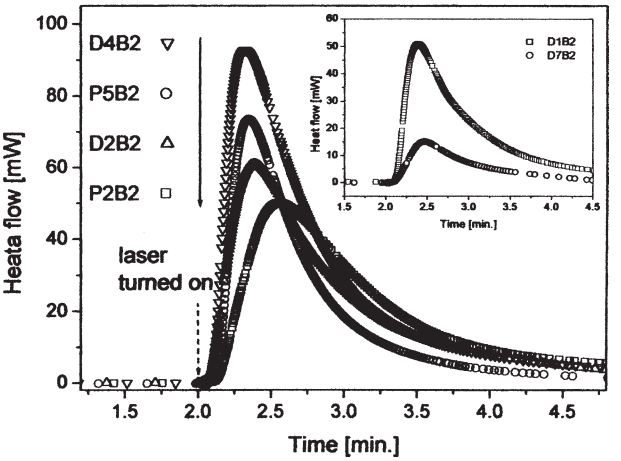

Figure 6 The family of kinetic curves recorded during the measurements of the flow of heat for the photoinitiated polymerization of the TMPTA/MP (9/1) mixture initiated by the tested borate salts, $I_a = 100$ mW/cm^2. The applied dyes possess various chromophores and identical borate anion. Inset: photopolymerization kinetic traces for the polymerization initiated by mono- (D7B2) and dicationic (D1B2) hemicyanine borate salts.

Photoinitiating abilities

Photoredox pairs consisting of the homodicationic hemicyanine dyes (acting as electron acceptor) and the *n*-butyltriphenylborate anion (acting as electron donor) were tested as photoinitiating system for the polymerization of a multiacrylate monomer. Since the maximum of the absorption band of the tested dyes is located in the range of 460–565 nm, for the photoinitiation of the polymerization the emission of an argon-ion laser emitting at 514 nm (Melles Griot) was used. The kinetic curves obtained for the polymerization of TMPTA-MP (9 : 1) mixture recorded for tested hemicyanine borate salts as photoinitiators, under the irradiation with a visible light, are shown in Figure 6 for illustration.

The rates of photoinitiated polymerization estimated for all tested photoredox pairs are collected in Table II.

It is apparent from the inspection of the rates of polymerization that the photoinitiation efficiency of the tested photoinitiators depends strongly on their structure. The highest rates of photoinitiated polymerization were observed for the bischromophoric dyes based on quinoline heterocycle. Additionally, it was found that the photoinitiation efficiency of the tested hemicyanine borates depends on a character of dialkylamino substituent in the electron donating part of the molecule. The best photoinitiating abilities exhibit the photoredox pairs possessing diphenyl- (**P4B2**, **P5B2**, **P6B2**, and **D4B2**) amino substituents in the dye molecule (see data in Table II). Generally, the initiators that couple two electron donors in one molecule of a photoinitiating dye exhibit significantly higher rate of polymerization in comparison with the model, mono-charged, hemicyanine dye. This conclusion was drawn from the results obtained for the experiments in which the entire light emitted by argon-ion laser was absorbed by the dye. This, in turn, was controlled by the concentration of photoinitiators (see Fig. 9).

The initiation of the polymerization via the photoinduced intermolecular electron transfer process involves many steps, including the photoinduced electron transfer from an electron donor to the excited state of the dye or from an excited electron donor to ground state of electron acceptor followed by secondary reactions, which yields a neutral radical initiating polymerization.

The steps determining the reaction rate of the radical initiated polymerization via intermolecular electron transfer process (PET) are dependent on the nature of the dye and the electron donor (or acceptor). In the case of alkyltriphenylborate salts, as the electron donor, the alkyl radical is formed as a result of the rapid cleavage of the alkyl boron bond of the boranyl radical obtained as a result of the photoinduced electron transfer from borate anion to the excited state of an electron acceptor.[11,31,32] According to Chatterjee's et al. studies on symmetrical cyanine borate initiators,[31,32] in nonpolar or medium polarity solvents, one can treat cyanine cation and borate anion as an ion pair. However, our studies on the influence of the borate anion concentration on the rate of photoinitiated polymerization indicates, for identical monomer-dye formulation, a distinct increase in the rate of polymerization as the concentration of borate anion increases.[15–17] This finding

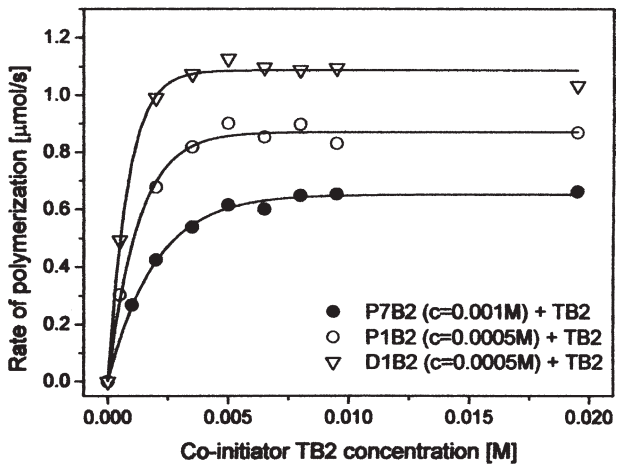

Figure 7 Dependence of the rate of photoinitiated polymerization on concentration of the electron donor (TB2). The type of dye is marked in the figure.

suggests that at the concentration of borate anion equals to the concentration of cyanine cation, only a part of the photoredox pairs exist as the ion pair. Since the electron transfer for cyanine dyes occurs on their singlet state, the existence of cyanine cation and borate anion as an ion pair is the basic prerequisite for the effective electron transfer. It is obvious that the additional amount of the borate anion in polymerizing composition should shift the equilibrium between free ions—ion pair to the higher concentration of the ion pair and causes an increase of the photoinitiation efficiency of dye-borate salt. It seems to be obvious that also an artificial increase of an electron donor in one molecule achieved by the coupling of second borate anion to the dye molecule should improve photoinitiating ability of tested compounds. Our experiments confirm this suggestion. From the inspection of the data collected in Table II, it is clear that the rate of polymerization initiated by asymmetric hemicyanine—borate pairs increases for double charged dyes. This finding suggests that one can treat homodicationic hemicyanine cation and borate anion in nonpolar or medium polarity solvents as an ion pair. However, a more precise study on the influence of borate concentration on the rate of photoinitiated polymerization indicates that under conditions created by the polymerized formulation (medium viscosity and medium polarity), one observes a distinct increase in the rate of photopolymerization as the concentration of borate anion increases. Figure 7 illustrates this relationship. On the basis of this experiment, it appears that at the experimental condition, only a part of photoredox pairs exist as an ion pair. Detailed analysis of the data presented in Figure 7 indicates that for **P7B2** initiating system only about 23% and for **P1B2** and **D1B2** initiating system as much as 35 and 44% of photoredox couples, respectively, exist as ion pairs. At concentration of the dye equal 1×10^{-3} *M* for monochromophoric and 5×10^{-4} *M* for bichromophoric photoinitiators, these values give an equilibrium constant of $\sim 2.65 \times 10^{-3}$ *M* for **P7B2**, 6.18×10^{-4} *M* for **P1B2**, and 3.63×10^{-4} *M* for **D1B2**, respectively.

One more interesting feature of the tested dyes is worthy of attention. As previously reported for the alkyltriphenylborates,[11,31,32] the rates of alkyl radical formation, as the result of the boranyl radical decomposition, are directly related to the stabilities of the alkyl radicals formed. Since the decay of the boranyl radical is found to be very fast and irreversible, the rate of back electron transfer is negligible.[33] Therefore, the efficiencies of alkyl radical formation and, hence, the initiation of the polymerization depend on the observed efficiency of electron transfer from the borate anion to the singlet state of cyanine molecule.

The Marcus theory[34,35,36]allows to predict the rate of the primary process, e.g., the rate of the photoinduced electron transfer process. The use of cyanine borate creates a unique opportunity to study the possibility of the application of this theory for the description of the rate of polymerization via an intermolecular electron transfer process. For these dyes, the change of the driving force of the electron transfer process has no influence on the type of the yielding free radical.

In our earlier articles,[11,15–17] we have shown that in the very viscous media, the rate of polymerization initiated via a photoinduced intermolecular electron transfer can be described as follows:

$$\ln \mathrm{Rp} = \mathrm{A} - (\lambda + \Delta \mathrm{G_{el}})^2 / 8\lambda \mathrm{RT} \qquad (6)$$

where A for the initial time of polymerization is the sum: $\ln k_p - 0.5 \ln k_t + 1.5 \ln[\mathrm{M}] + 0.5 \ln I_a$ (here k_p, k_t denote the rate constant of polymerization and termination respectively, [M] is the monomer concentration, I_a is intensity of absorbed light), λ is the reorganization energy necessary to reach the transition states both of excited molecule and solvent molecules.

Equation 6 clearly indicates that if the primary process, e.g., the rate of electron transfer process controls the observed rate of photopolymerization, one should observe a parabolic relationship between the logarithm of polymerization rate and the free energy change ΔG_{el}. For the photoinitiating photoredox paris examined, it is shown in Figure 8.

It is apparent from the inspection of the relationships presented in Figure 8 that the plot exhibits predicted by Marcus or more likely by the Rehm–Weller[30] and Agmon–Levine[37] equations. It seems to be obvious that for the tested initiating photoredox pairs, two independent curves should be observed.

According to Figure 8, the rate of radical polymerization initiated by the series of hemicyanine borates increases as the driving force of the electron transfer reaction increases. This behavior is predicted by the classical theory of photoinduced electron transfer.[38,39]

The concentration of photoinitiator also plays a key role in the photopolymerization. In the conventional UV–Vis photopolymerization, R_p increases when more of the initiator is used, up to a certain level, than rapidly decreases when too much initiator is added to a polymerizing formulation. This behavior is attributed to the "internal filter effect." This property becomes more significant for photoinitiators with high-molar absorption coefficient.[15–17,40]

Figure 9 presents the relationship between the rate of polymerization and the concentration of photoinitiator. It is evident that as the photoinitiator concentration is increasing, the rate of polymerization increases and reaches a maximum followed by continuous mild decrease. For the tested photoinitiators with two electron donors in one molecule, the highest rates of polymerization (for 1-mm thick sample; Fig. 9) were achieved at the initiator concentration of about 1×10^{-3} *M* and 5×10^{-4} *M* for series D and P, respectively. The reduction of the photoinitiated polymerization rate at high initiator concentration, for applied technique of the polymerization rate measurement, can be easily understood taking into account the decrease of the penetration depth of the laser beam being a result of so-called the "internal filter" effect.[15–17,40]

CONCLUSIONS

Asymmetric cyanine dyes, modified in a way allowing introducing to their structures an additional organic cation were applied as visible-light photoinitiators of vinyl monomers polymerization. The tested homodicationic chromophores, when coupled with *n*-butyltriphenylborate anions, show significantly enhanced photoinitiation ability in comparison with their monocationic analogues. This is attributed to an artificially increased concentration of the *n*-butyltriphenylborate anion (acting as electron donor), in proximity to the electron accepting excited cyanine dye chromophore. The artificial increase of an electron donor concentration in the photoinitiator molecule causes, both, the decrease in the dissociation constant and the enhancement of the photoinitiating abilities of the photoredox pair. The rate of photoinitiation is also affected by the structure of the hemicyanine cation.

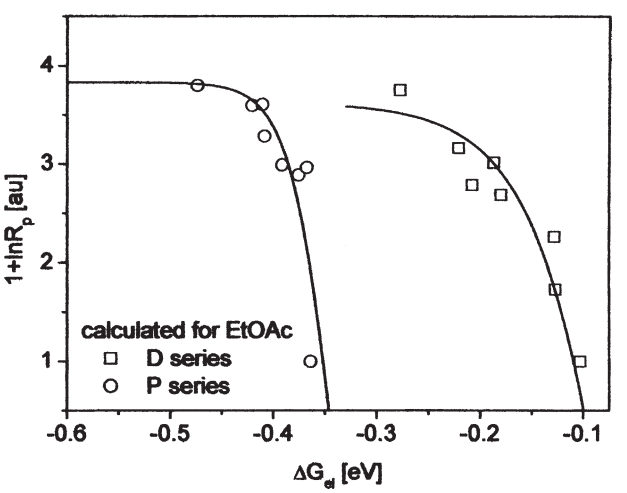

Figure 8 Dependence of the rate of photoinitiated polymerization on the free energy (ΔG_{el}) for the photoinduced electron transfer process from borate to the excited state of bischromophoric cyanine dye.

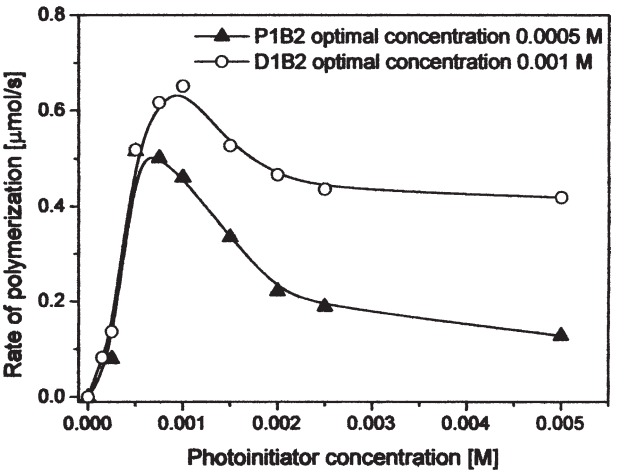

Figure 9 Rate of the polymerization versus photoinitiator concentration.

We would like to express our gratitude to Professor Jerzy Pączkowski for participation in discussion and preparation of the article.

References

1. Pappas, S. P. UV Curing Science and Technology; Technology Marketing, Corp.: Norwalk, CA, 1978.
2. Fouassier, J. P. Photoinitiation, Photopolymerization and Photocuring; Hanser Verlag: Munich, 1995.
3. Dietliker, K. Chemistry and Technology of UV and EB Formulation for Coatings, Inks and Paints, Vol. 3; Technology, Ltd./SITA: London, 1991.
4. Davidson, R. S. Exploring the Science, Technology and Applications of UV and EB Curing; SITA Technology, Ltd.: London, 1999.
5. Mishra, M. K.; Yagci, Y. In Handbook of Radical Vinyl Polymerization; Marcel Dekker, Inc.: New York, 1998.
6. Ledwith, A.; Purbrich, M. D. Polymer 1973, 14, 521.
7. Davidson, R. S. In Advances in Physical Chemistry; Bethel, D., Gold, V., Eds.; Academic Press: London, 1983.
8. Ledwith, A.; Bosley, J. A.; Purbric, M. D. J Oil Col Chem Assoc 1978, 61, 95.

9. Linden, L.-Å.; Pączkowski, J.; Rabek, J. F.; Wrzyszczyński, A. Polimery 1999, 44, 161.
10. Kabatc, J.; Kucybała, Z.; Pietrzak, M.; Ścigalski, F.; Pączkowski, J. Polymer 1999, 40, 735.
11. Kabatc, J.; Pietrzak, M.; Pączkowski, J. Macromolecules 1998, 31, 4651.
12. Kabatc, J.; Jędrzejewska, B.; Pączkowski, J. J Polym Sci Part A: Polym Chem 2003, 41, 3017.
13. Kabatc, J.; Jędrzejewska, B.; Pączkowski, J. J Appl Polym Sci 2006, 1, 207.
14. Kabatc, J.; Pietrzak, M.; Pączkowski, J. J Chem Soc Perkin Trans 2002, 2, 287.
15. Kabatc, J.; Kaczorowska, M.; Jędrzejewska, B.; Pączkowski, J. J Appl Polym Sci 2008, 108, 1636.
16. Jędrzejewska, B.; Jeziórska, J.; Pączkowski, J. J Photochem Photobiol A: Chem 2008, 195, 105.
17. Jędrzejewska, B.; Marciniak, A.; Pączkowski, J. Mater Chem Phys 2008, 111, 400.
18. Jędrzejewska, B.; Kabatc, J.; Pączkowski, J. Dyes Pigm 2007, 73, 361.
19. Jędrzejewska, B.; Kabatc, J.; Pączkowski, J. Dyes Pigm 2007, 74, 262.
20. Jędrzejewska, B.; Rudnicki, A. Dyes Pigm 2009, 80, 279.
21. Brandrup, J.; Immergut, E. H. Polymer Handbook, 3rd ed.; Wiley: New York, Chichester, Brisbane, Toronto, Singapore, 1989; p II/298.
22. Mishra, A.; Behera, R. K.; Mishra, B. K.; Behera, G. B. J Photochem Photobiol A 1998, 116, 79.
23. Koti, A. S. R.; Bhattacharjee, B.; Haram, N. S.; Das, R.; Periasamy, N.; Sonawane, N. D.; Rangnekar, D. W. J Photochem Photobiol A Chem 2000, 137, 115.
24. Loew, L. M.; Simpson, L. L. Biophys J 1981, 34, 353.
25. Ephardt, H.; Fromherz, P. J Phys Chem 1989, 93, 7717.
26. Lakowicz, J. R. Principles of Fluorescence Spectroscopy; Plenum: New York, 1983; p 266.
27. Lippert, E. Z Naturforsch Teil A 1955, 10, 541.
28. Mataga, N.; Kaqifu, Y.; Kouzumi, M. Bull Chem Soc Jpn 1955, 28, 690.
29. Mishra, A.; Behera, G. B.; Krishna, M. M. G.; Periasamy, N. J Luminesc 2001, 92, 175.
30. Rehm, D.; Weller, A. Ber Bunsen-Ges Phys Chem 1969, 73, 834.
31. Chatterjee, S.; Gottschalk, P.; Davis, P. D.; Schuster, G. B. J Am Chem Soc 1988, 110, 2326.
32. Chatterjee, S.; Davis, P. D.; Gottschalk, P.; Kurz, M. E.; Sauerwein, B.; Yang, X.; Schuster, G. B. J Am Chem Soc 1990, 112, 6329.
33. Schuster, G. B. Pure Appl Chem 1990, 62, 1565.
34. Marcus, R. A. J Chem Phys 1956, 24, 966.
35. Marcus, R. A. J Chem Phys 1963, 67, 853.
36. Marcus, R. A. J Chem Phys 1965, 43, 679.
37. Agmon, N.; Levine, R. D. Chem Phys Lett 1977, 52, 197.
38. Eberson, L. Electron Transfer in Organic Chemistry; Springer-Verlag: New York, 1987.
39. Pączkowski, J.; Neckers, D. C. Photoinduced Electron Transfer Initiating Systems for Free Radical Polymerization, In Electron Transfer in Chemistry; Balzani, V., Ed.; Wiley-VCH: Weinheim, 2001; Vol. 5, pp 516.
40. Zhang, S.; Li, B.; Tang, L.; Wang, X.; Liu, D.; Zhou, Q. Polymer 2001, 42, 7575.